JCSE The Journal of Corrosion Science and Engineering
ISSN 1466-8858 Volume 16, Preprint 68 submitted 27 November 2013

Eco-Friendly Nano-Hybrid Coatings for the Protection of Bio-Fouling

P. Saravanan[1], D. Duraibabu[2], S. Ananda Kumar[3]

[1]*Department of Chemistry, St. Joseph's College of Engineering, Chennai 600119, India.*

[2,3]*Department of Chemistry, Anna University, Chennai 600025, India.*

Abstract

Epoxy nano-composite coating was developed using amine functionalised nZnO (in the amount of 2.5%, 5.0% and 7.5wt %) as dispersed phase and a commercially available epoxy resin as matrix phase. The structural features of these materials were ascertained by FT-IR spectral studies. The anti-corrosive properties of the epoxy/nZnO hybrid coatings in comparison with a virgin coating were investigated by salt spray test and electrochemical impedance spectroscopy technique. The surface morphological images were taken by SEM indicate that nZnO particles were dispersed homogenously through the epoxy polymer matrix. The results showed improved antifouling and anticorrosive properties for epoxy-nZnO hybrid coatings.

Keywords: A. Mild steel; A. Zinc; B. IR Spectroscopy; B. EIS; B. SEM; C. Polymer coatings.

*Corresponding author. Tel.: +91-44-24501060

E-mail address: saranpava@gmail.com (P. Saravanan)

ISSN 1466-8858 Volume 16, Preprint 68 submitted 27 November 2013

1. Introduction

The ban on harmful substances in antifouling paints paved an avenue to the development of new antifouling strategies. Alternative coatings should be as effective as conventional paints but with lower toxicity. Bio fouling is the accumulation of micro-organisms, plants and animals on surfaces [1] causing serious damage and fuel consumption, which may be as high as 7% of GDP. To overcome these drawbacks of fouling and to further improve the performance of coatings, incorporation of nano-sized pigments and fillers in the coating is a recent practice. The most common nano-particles used in coatings are SiO_2, TiO_2, ZnO, Al_2O_3, $CaCO_3$, etc. nZnO due to its characteristic structure possesses unique chemical, biological and semi-conductor properties. Because of its non-toxic nature and ability to block UV radiation, it has found vast applications in cosmetics, textile and in many coating industries [2-4].

On the other hand, dispersion of nanoparticles into polymer matrix is a challenging task, which often involves agglomeration of nanoparticles leading to poor performance of coatings. The surface of nanoparticles must be modified with suitable coupling agent to ensure its perfect dispersion and to prevent the agglomerated nanoparticles. Many studies have been done toward the organized fabrication of surface functionalization of nanoparticles through organoalkoxysilanes [5-9]. Functionalization of nanoparticles prevents desegregations during curing, resulting in a more homogenous coating. Moreover, nanoparticles tend to occupy small hole defects formed from local shrinkage during curing of the resin and act as a bridge as well interconnecting more molecules. These results in an increase in the rigidity of coatings leading to improved barrier

ISSN 1466-8858 Volume 16, Preprint 68 submitted 27 November 2013

properties required for corrosion and fouling protection and reduce coating blister formation or delamination [10-13].

In this work, surface modification of nZnO was achieved with 3-aminopropyltriethoxysilane coupling agent and the surface modified nZnO in different concentrations was reinforced with epoxy resin to formulate nZnO reinforced epoxy coatings. The reinforcing effect of nZnO particles with epoxy resin towards corrosion and fouling resistance was investigated by several techniques such as Fourier transform infra-red (FTIR) spectra, electrochemical impedance (EIS), salt-spray test, SEM and field exposure study. The mechanical properties of the nZnO reinforced epoxy coatings along with virgin epoxy coating were determined by flexibility test, cross-cut adhesion test, impact resistance test [14-20]. The data resulted from the study is elaborated in detail with supporting evidences.

2. Experimental

2.1. Materials

Epoxy resin GY250 representing diglycidyl ethers of bisphenol-A (DGEBA) with Epoxy equivalent weight (EEW) 182-192 (E.wt/g) and viscosity about 10,000 mPa was used for our study. Aradur HY951 curing agent was obtained from Huntsman (India). The Silica powders, red iron oxide pigment, nZnO and 3-aminopropyltriethoxysilane were purchased from Aldrich Chemicals. Acetone, sulphuric acid, NaOH purchased from Sisco Research Laboratories, India. Rustoline oil, epoxy type adhesive (supplied by Hindustan Ciba-Geigy Ltd., India).

ISSN 1466-8858 Volume 16, Preprint 68 submitted 27 November 2013

2.2. Preparation and Testing of coatings

Mild steel specimens [of composition C-0.033%; Si-0.005%; Mn-0.235%; P-0.011%; S-0.005%; Cr-0.046%; Ti-0.003%; Ni-0.043%; Al-0.073%, Co-0.007%, Nb-0.005, Fe-balance] were used for our study. Five different coating systems used to protect steel structures against corrosion were chosen for the purpose of the research. The nomenclature of different coating systems is given in Table 1. The specimens were degreased with acetone to remove impurities from the substrate. Then the specimens were subjected to sand blasting at a pressure of 100 psi through the nozzle to get the appropriate crevice. The particle size of the sand is 82 meshes. The distance between the substrate and the blaster was maintained 2 feet. The specimens were kept in the rustoline oil for conditioning. The process of the preparation of hybrid coatings is shown in Figure1.

Coatings were applied by hand bar coater on commercially available mild steel plates (30mm x 10mm x 1mm) for chemical resistance test, 70mm x 50mm x 1mm for salt spray test. All the coated samples were cured at room temperature for 3 days and then kept in desiccators for at least 1 week before the tests were performed. Coating thickness was measured by Mini test 600FN, EXACTO-FN type. The thickness of the coatings was found to be approximately ±100µm. Before subjecting them to various tests, the panels were edge-sealed to an extent of 5-8mm from the edges using an epoxy type adhesive (supplied by Hindustan Ciba-Geigy Ltd., India).

2.3. Surface modification of ZnO nanoparticles:

The introduction of reactive NH_2 group onto the surface of ZnO nanoparticles was achieved through the reaction between 3- aminopropyltriethoxysilane and the hydroxyl

ISSN 1466-8858 Volume 16, Preprint 68 submitted 27 November 2013

groups on the ZnO nanoparticle surface. Typically, 2.0g ZnO nanoparticles and 2ml 3-aminopropyltriethoxysilane in 40ml O-xylene were kept at 150°C for 3hrs under stirring and Argon protection. After that, the ZnO nanoparticles were collected by filtration and rinsed three times with acetone. Afterwards, the amine functionalized ZnO nanoparticles were dried under vacuum for 12hrs. The reaction sequence is given in Scheme 1.

2.4. Preparation of epoxy resin / nano-ZnO /curing agent system

Prior to curing, the desired amount of epoxy resin, red iron oxide pigment, silica powder, leveling agent GLP503A and nZnO were mixed together and crushed followed by sifting through 200 mesh screen. The mixing process was performed in an oil bath (50-70^{0}C). The mixture was then subjected to ultra-sonication for 8-12h to disperse the nano particles of ZnO completely within the epoxy resin to fabricate antifouling coating after addition of stoichiometric amount of hardener to mixture. By this method, four coating formulations containing different amount of nZnO (2.5, 5.0 and 7.5wt. %) were prepared and the composite paint was applied on mild steel coupons using a bar-coater to a thickness of approximately ±100 µm. The surface modification of nZnO and its subsequent reaction with epoxy is illustrated in Scheme 2.

2.5 Spectroscopy Characterization

PerkinElmer 1750 FTIR spectrometer determines the chemical structure of virgin epoxy resin, nZnO modified epoxy resin and commercial epoxy resin. The spectra of epoxy resins cured with Aradur HY951 as coatings were obtained by the following method: a

ISSN 1466-8858 Volume 16, Preprint 68 submitted 27 November 2013

small portion of the cured epoxy resin was ground to a fine powder, mixed with KBr powder, and pressed into a pellet which is used to obtain the spectrum.

2.6 Mechanical properties

Impact resistance, Flexibility and Cross-Cut adhesion test [21-23].

(1) Impact resistance: To determine the impact indentation on the coated metal panels, the steel ball of about 50mm diameter and weighing 500±10g was dropped on the surface of the panel freely from a height of 750mm at randomly selected 10 different points on the surface avoiding nearness of edges as per ASTM D2794 and results are given in Table 2.

(2) Flexibility: This test which enables the measurement of resistance to cracking (flexibility) was carried out on all coated specimens as per ASTM D522 standard using a conical mandrel and results are given in Table 2.

(3) Cross-Cut adhesion test: Square boxes of $1mm^2$ were made on a 1cm X 1cm square of the test specimen. These boxes were covered by adhesive tape (cellotape). Cellotape was then pulled off and the number of boxes removed from the surface was counted to check the adhesion of the coating. Cross-cut adhesion was carried out according to ASTM 3359-83B and results are given in Table 2.

2.7 Water absorption and gel content measurement

The water absorption (w%) measurements for different epoxy/nZnO hybrid films of 3cm×1 cm size was calculated in a vacuum oven for 24 h to determine their dry weight (Wa) and water absorption was measured by immersing the film in distilled water for 24 h

ISSN 1466-8858 Volume 16, Preprint 68 submitted 27 November 2013

to determine the wet weight (Wb). Then the water absorption was calculated by the following formula [24].

$$W(\%) = \frac{Wb - Wa}{Wa} \times 100$$

A known weight of oven-dried film (W_1) was put into a Soxhlet extractor for continuous extraction with toluene for 24 h at 100^0C. The polymer gel remained after extraction was dried (W_2) and the degree of crosslinking was measured in terms of gel content (%). Three test specimens were used for each sample and the average was taken as gel content [25, 26].

$$\text{Gel Content}(\%) = \frac{W_2}{W_1} \times 100$$

2.8 Chemical resistance test

Corrosion test was performed in distilled water, acid (10 wt. % HCl), alkali (5 wt. % NaOH) and distilled water by placing the coated and uncoated specimens in individual plastic jars and dipping them in aforementioned media. The duration of the test was 96 days at 38^0c. The degree of adhesion and visual inspection of blister and cracks were evaluated for the coated panels. Acetone double rub test according to ASTM D 4752 was carried out to evaluate the chemical resistance of the coated samples [27, 28].

2.9 Salt spray test

An accelerated salt spray corrosion test was carried out on all coated steel panels of 70mm × 50mm × 1mm with and without diagonal scribes on coated panes. Salt spray tests were used to simulate the marine atmosphere where mild steel was exposed according to ASTM B 117-3. 5% NaCl solution was made and used as salt spray solution

with a pH of 6.9, air pressure of 15psi. A scratch with 200 µm in width and 40 mm in length was made. The temperature of the salt spray chamber was controlled between 33.8-35.1^{0}C, with a continuous test time of 1200hrs. The method followed for cleaning the specimen before loading and after completion of testing as follows: a) Specimen cleaned gently prior to loading: b) Specimen washed gently in clean running water to remove salt deposits from their surfaces and then dried immediately. The panels were carefully observed for the detection of rust spots on their surface and photos were taken by Olympus 4XWIDE digital camera. The time for the formation of brown rust and blisters was noted [29-31].

2.10 Potentiodynamic polarization measurement

In the case of Tafel polarization, potential was scanned from-250mV to +250mV with respect to open circuit potential (OCP) at a scan rate of 0.5mV/Sec. From this anodic and cathodic polarization curves, the Tafel regions were identified and extrapolated to E_{cor} to get corrosion potential I_{cor} and corrosion rate CR in mm per year [32]. All measurements were carried out at ambient temperature (25±2^{0}C). The experimental data were analyzed by using the commercial software package ZSimpWin [33-40]. The interpretation of impedance data was performed after numerical fitting using an equivalent circuit proposed in Figure 2(b).

2.11 Electrochemical impedance spectroscopy (EIS)

EIS measurements were performed on a three electrode corrosion cell by an ACM electrochemical impedance analyzer (Gill AC Serial No. 1634- Sequencer Version 4). A saturated calomel electrode (SCE) and platinum foil were used as reference and counter electrodes, respectively. For electrochemical impedance spectroscopy experiments, mild

ISSN 1466-8858 Volume 16, Preprint 68 submitted 27 November 2013

steel substrates with the dimensions of 3cm x 1.4cm x1cm were used. These panels were sand blasted and cleaned with ethanol in an ultrasonic bath before painting. The sand blasted panels were painted by a hand bar coat applicator and the coated specimens were dried for 12h at ambient temperature. The dry film thickness measured was found to be approximately ±100µm for all the coated specimens. The EIS test was performed in 3.5% sodium chloride electrolyte solution. Only 1cm^2 area of the uncoated specimen, pure epoxy coated specimens and nZnO-epoxy coated specimens were exposed to the electrolyte. The remaining areas were sealed by a masking tape. In electrochemical impedance spectroscopy experiment, ac signal of 10mV amplitude and various frequencies from 10000 Hz to 0.1Hz at open circuit potentials were impressed to the coated mid steel samples. Figure 2(a) represents the typical test setup for the EIS study of the coated specimens. From the impedance plots, the charge transfer resistance, R_{ct} and the double layer capacitance, C_{dl} values can be calculated.

2.12 Field exposure test at Muttukadu, India

Mild steel specimens (of 8cm x 5 cm x 1 cm) coated with unmodified epoxy, nZnO containing epoxy coating systems were used for the fouling study. The study was carried out at coast of Bay of Bengal in Chennai, on the East Coast of India. The specimens were suspended at a depth of 3m from the lowest spring tide low water mark. The specimens hung vertically using nylon ropes with proper support in a protected area for 365 days. The specimens were removed and the distribution of fouling growth to observe the corrosion associated with fouling. The barnacles, along with other organisms, which settled on the surface of specimens coated with different coating systems, where then, removed using a hard brush without damaging the specimen surface [41, 42].

ISSN 1466-8858 Volume 16, Preprint 68 submitted 27 November 2013

2.13 SEM analysis

The same samples were then coated with a thin layer of gold by vaporization and morphology of antifouling coating panels was observed by scanning electron microscope (LEO 1455VP). Samples were examined before and after degradation by immersion in the marine environment [43-45].

3. Result and Discussion

3.1. FTIR analysis of the epoxy/ZnO nanocomposite coatings

The structures of GY250 epoxy resin and HY951 polyamine adducts were confirmed by IR spectral analyses. The six different coating formulations exhibit very different IR spectra. The IR spectrum of GY250 reveals the presence of characteristic absorption bands for Ar–C=C–H stretching and bending $–CH_2$ and $–CH_3$ asymmetrical and symmetrical, –C–Ar–O–C stretching, and epoxy CH_2–(O–CH–) ring stretching vibration. The presence of epoxy groups in IR spectra was proved from the presence of strong bands at 3056 cm^{-1} (γC-H epoxy) and 915 cm^{-1} (γC-O epoxy). The 1, 4-substitution of aromatic ring was seen at 830cm^{-1} for GY250 epoxy resin. There was a broad band with very low intensity at 3429cm^{-1} corresponding to the vibration mode of water OH group indicating the presence of small amount of water adsorbed on the nZnO crystal surface. The band at 1601 cm^{-1} was due to the OH bending of water. A strong band at 530cm^{-1} is attributed to the nZnO stretching band which is consistent with that reported before. The IR analysis carried out for HY951 polyamine adducts reveals the presence of characteristic absorption bands for N–H stretching and bending vibration. The broad doublet peak observed between 3340–3200 cm^{-1} may be due to the $–NH_2$ vibration absorption of amine compound. The aliphatic $–CH_2$ and $–CH_3$ vibrations were seen between 3000 and

ISSN 1466-8858 Volume 16, Preprint 68 submitted 27 November 2013

2850cm^{-1} for the polyamine adduct. The most obvious distinguishing features were that the polyamine adduct spectra had an intense broad N–H stretching absorption around 3300 cm^{-1} [46-54]. Figure 3 shows the infrared spectra of all the coatings analyzed on KBr disc between the zone 400–4000 cm^{-1}.

3.2. Analysis of mechanical properties

Though flexibility test is not quantitative in nature, it provides qualitative results on the coating systems. Results of the impact test carried out on all coatings indicate that all the coatings have passed the impact test. Results of conical mandrel flexibility test conducted on all the coatings are shown in Table 2, bring out the fact that Coating '1' failed at 3mm diameter of the cone where peeling and cracks were predominantly found and passed at 6mm diameter. All other coatings have been found to possess good flexibility characteristics. The failure of coating '1' may be attributed to the formation of large free volumes, micro voids and stress concentration during the film formation [55-57].

The adhesion of coating depends on the nature of substrates as well as on the coating formulations. Table 2 shows the results of adhesion tests of virgin epoxy and epoxy coatings containing nZnO. From the test, we observed that no squares were removed from the coated metal substrates except coating '1' whose squares were removed (3-4 in numbers) during cross-cut adhesion test. These results indicate that the adhesion of epoxy/nZnO hybrid coatings was superior to the virgin epoxy coating [58]. The reason for the improved adhesion offered by epoxy/nZnO hybrid coatings may be due to their enhanced integrity and flawless nature.

3.3. Results of water absorption and gel content test

ISSN 1466-8858 Volume 16, Preprint 68 submitted 27 November 2013

The data in Table 2 show that the minimum water absorption and maximum (%) of gel content for coatings having increasing nZnO content. This may be due to the more cross linked structures formed with increased nZnO content. The incorporation of nZnO particles into epoxy resins offers enhanced integrity and durability of such coatings, since these fine particles dispersed in coatings seem to have occupied cavities and caused crack bridging, crack deflection and crack bowing. Functionalization of nanoparticles also prevented epoxy disaggregation during curing, resulting in a more homogenous coating. Moreover, nZnO occupy acted as a bridge, interconnecting more molecules leading to a reduced total free volume and increased cross linking density and rigidity [59-61].

3.4. Analysis of Chemical resistance test

In the previous section we have discussed the mechanical tests of the cured nano-composite coatings '1' to'5'. In the present section, we have discussed the chemical resistance of Nano-composite coatings '1' to '5'. For the chemical resistance test, the coated panels were subjected to adverse chemical environments such as acid, alkali, solvent and water in order to study the durability of such coatings. The data obtained for cured coating systems (virgin and composite coatings) from water, acid, alkali, and solvent exposure were listed in Table 3. The uncoated panels underwent minimum weight loss in water while coated panels (mild steel, Table 3) remained unaffected in aqueous medium (distilled water) indicating that these coating materials render an impermeable barrier to the substrates of mild steel through which water and other corrosive species could not enter and thus they successfully protected the substrate from corrosion. Furthermore, the immersion of these composite coated specimens in 5wt% H_2SO_4 and 5wt% NaOH for 96h had their films remained intact with a slight loss in gloss. The better

ISSN 1466-8858 Volume 16, Preprint 68 submitted 27 November 2013

performance shown by nZnO reinforced epoxy amine cured coatings may be attributed to their increased cross linking density, which was achieved by crack bridging leading to enhanced integrity of such coatings [61-62]. The uncoated panels underwent maximum corrosion under 5wt% NaOH solution, which was evident from their weight loss measurements (Table 3). However, all coated samples were found to be quite resistant to water, acid, and alkali environment.

The use of polar solvents such as ketones is often used to assess the degree of cure of a cross-linked composition for solvent resistance, methyl isobutyl ketone or acetone is recommended. In addition to immersion testing, solvent resistance may be assessed by a solvent rub rest. In this respect, acetone was used to determine the degree of curing of the present coating systems by rub method. The failure of tests was determined either by distruption or dissolution of the coating films from panels. Higher the degree of cross-linking better the film properties ideally required for corrosion resistance. Hence solvent molecules can hardly penetrate the cross-linked network at all. In this respect, it was found that the all developed composite coatings pass acetone double rub test and there was no defect on the surface even after 27 double rubs of solvent indicating their superior performance than uncoated specimens.

3.5. Evaluation of corrosion resistance by potentiodynamic polarization studies

Figure 4 shows typical potentiodynamic polarization curves for mild steel in 3.5% NaCl with and without coating of paint. It was apparent that the polarization curves for mild steel coated with paints showed remarkable potential shifts to noble values compared to the uncoated metal immersed in 3.5% NaCl. The various polarization parameters such as

corrosion potential (E_{corr}) and corrosion current density (I_{corr}) obtained from cathodic and anodic curves by extrapolation of Tafel lines are given in Table 4. It should mentioned that the E_{corr} values increased significantly for mild steel coated with the coatings '3', '4', '5', '2', '1' and uncoated mild steel. This observation clearly showed that mild steel applied with these coatings control both cathodic and anodic reactions and thus act like mixed type inhibitors [63]. For instance, the corrosion rate for uncoated mild steel was found to be 1.0298×10^{-1} mm/y and it was minimized by coating the metal with coating '3' to a lower value of 1.4960×10^{-6} mm/y than the other coatings namely coating '1', '2', '4' and '5' whose values are respectively 2.07677×10^{-3}, 9.3727×10^{-3}, 3.8113×10^{-3}, 2.5744×10^{-3}. Moreover, the CR of coating '3' is found to be very minimum i.e. 1.4960×10^{-6} mm/year, which is 10% lower than that observed for uncoated MS. Hence it was observed that the coatings applied on mild steel restrict the interaction between the metal and the electrolyte to a considerable extent. The extent of restriction to the entry of corrosive species was more in the case of coating '3' and least in the case of coating '1' and uncoated specimens. The reason for this behavior exhibited by coating '3' may be due to the even distribution of 2.5 wt% nZnO within the epoxy coating offering barrier effect by interconnecting more molecules leading to a defect free coating.

3.6. Evaluation of corrosion resistance by EIS

The Bode plots for the uncoated mild steel and coating systems '1', '2', '3', '4' and '5' are depicted in Figure 5. EI Studies were carried out on mild steel panels coated with modified epoxy resin containing with and without nZnO in 3.5%NaCl. It was interesting to note that except uncoated mild steel and neat coating, all modified epoxy coated samples with and without nZnO showed corrosion resistance up to 10^3-10^8 Ohm.cm^2

ISSN 1466-8858 Volume 16, Preprint 68 submitted 27 November 2013

indicating a moderate corrosion taking place initially and the results were depicted in Table 5 [64]. The impedance was analysed by using simple Randle's circuit, since one semicircle is obtained in the Nyquist plot. Since polymer coatings were low in many cases and the impedance behaviour represents the charge transfer process of the mild steel dissolution. From the Figure 5 and Table 5, it was clearly evident that the coating '3' having high corrosion resistance (1.071×10^{8}) to other coatings (uncoated, '1', '2', '4' and '5') with and without nZnO and the order of corrosion resistance is found to be as follows:

$$3 > 4 > 5 > 2 > 1 > \text{uncoated}$$

This superior corrosion resistance offered by coating system '3' may be due to the presence and even distribution of surface modified nano zinc oxide of optimum wt%, which gave a flawless coating of low porosity, high crosslinking density having improved coating integrity.

3.7. Salt spray test results

The coated specimens were subjected to diagonal scratch with the help of a sharp knife in order to expose the base metal to the continuous salt fog chamber containing 3.5% NaCl solution. The 1200 hours salt spray test supports the results obtained from EIS studies. The salt spray results of coated panels before and after exposure to salt fog atmosphere are schematically given in Figure 6. At the end of the salt spray test, no visible corrosion products were seen on the surface of the unscratched area of panels coated with modified epoxy coating '3' and '4'. As observed in the case of EIS, coating 1containing no nZnO and other additives offered poor corrosion resistance than other four coatings ('2', '3', '4' and '5') chosen for the study. The Table 6 shows the results of the observations made for

ISSN 1466-8858 Volume 16, Preprint 68 submitted 27 November 2013

the coatings '1' to '5' after 600 and 1200h of salt-spray test. The intact films showed neither corrosion nor coating defects on the main body of the panels. However, rusting without spreading was observed at the cross-scribe suggesting an impressive performance of the formulations against salt atmosphere [65, 66]. Hence all formulations gave good results without major loss of adhesion; blistering and rusting of the cross-cut even after 1200h of salt-spray exposure in the cabinet. However, coatings '1' being virgin epoxy and coating '2' exhibited poor salt-spray resistance. The order of corrosion resistance of all the coatings is given below:

$$3 > 4 > 5 > 2 > 1$$

3.8. Antifouling studies by scanning electron microscopy (SEM)

Fouling resistance of these coatings was determined by antifouling studies by subjecting the coated samples in sea for a period of 12 months at east coast of India, Tamil Nadu, Chennai (Muttukadu boat house). For SEM observation, sample were fixed in a glutaraldehyde solution then washed in a phosphate buffer. Dehydration has been performed in different alcohol/water solutions, followed by critical point drying of samples. SEM photographs of the '1', '2', '3', '4' and '5' coated specimens attached with fouling organisms were taken. The surface morphology of '1', '2', '3', '4' and '5' coated samples after immersion in sea for the evaluation of fouling was examined by SEM and the results are illustrated in Figure 7. From the fouling study, we observe that there was more corrosion on uncoated mild steel and more fouling attachment on coating '1', '2', and '5' respectively. On the other hand, the intensity of fouling organisms attached to '3' and '4' coated panels was minimum. Among the biocide loaded coated panels, specimen coated with coating '3' (2.5% nZnO) showed least fouling organisms on its surface than

ISSN 1466-8858 Volume 16, Preprint 68 submitted 27 November 2013

'1', '2', '4' and '5' coated specimens indicating its excellent antifouling ability. This may be due to its superior antimicrobial activity imparted by optimised coating formulation '3' than the other concentration [67]. The mechanism of foul release from amine functionalized nZnO surfaces is still not completely understood. However, it is generally believed that the anti-biofouling properties are due to their low surface energies. A similar observation was made by Chen et al. [68] for the low surface energy non-toxic organo silicon nano-SiO_2 antifouling coatings, which showed less the adhesions of the biofouling organisms on the coating films. The order of fouling resistance of all the coatings is given below:

3 > 4 > 5 >2 > 1 > uncoated

Figure 8 (a) shows the photographs of '1', '2', '3', '4' and '5' coated panels against fouling for 6 months immersion in the seawater exposure. The coating system '3' having better corrosion resistance than coating systems '1', '2', '4' and '5' resisting the adhesion of microorganisms and biofilms indicating their superior fouling resistance as well. Figure 8 (b) ('1', '2', '3', '4' and '5') shows the fouling resistance of the different coating systems immersed in seawater for 1 year. From this study, coating systems '3' was again determined to have less fouling organisms on the coated panels indicating their excellent antifouling performance required for marine industry. It can be seen that the antifouling efficiency of the coating film first is improved by adding 2.5wt% of nZnO and then the performance becomes worse when the amount of nZnO added is 5 wt% and 7.5 wt% respectively. The reason which caused this change of antifouling property may be inferred from the results. When the addition of nZnO is 2.5wt%, it is well distributed within the coating, to effectively inhibit bio-fouling. On the other hand, if the addition of n ZnO is beyond 2.5wt%, the excess addition causes uneven distribution of nZnO in the coating

ISSN 1466-8858 Volume 16, Preprint 68 submitted 27 November 2013

film which might have led to the pore formation on the surface of the coating namely '4' and '5'. This porous nature of the coating '4' and '5' favored the invasion by marine fouling organism's thus imparting inferior antifouling activity than coating '3'. Similar observation was made from EIS study where the coating '3' containing 2.5wt% of nZnO exhibited the best corrosion resistance indicating nZnO's even distribution within the epoxy matrix offering better coating integrity. Moreover, the fouling organisms attached to coated film '3' were removed very easily after the fouling test was over, and the panel looked fresh (photographic image of coated specimen after fouling test resembling the one before the test was performed. This observation further confirms the better antifouling performance of coating '3' in comparison with other coatings of the present study.

3.9 Mechanism of the property improvement

For nZnO have been well dispersed in the epoxy resin/nZnO composite through in situ and inclusion polymerization, they can also effectively be dispersed in the resultant nZnO modified coatings. After flowing and curing, the nanoparticles can be thoroughly dispersed in the coating films. Figure 9 shows the forming process of the nZnO modified coating films, and other normal sized fillers are ignored in order to describe it more clearly.

As shown in figure 9, the exist of nZnO can form extra interact point with epoxy resin beside curing point, which can enhance the compactness of the coating film and result in the improvement of neutral salt spray corrosion resistance of the coating films. When the coating films were distorted or impacted, inorganic particles will act as stress concentrator and craze will come into being at the interface. Because nanoparticles have advantages in quantity and specific surface areas at the same loading content compared with micron

ISSN 1466-8858 Volume 16, Preprint 68 submitted 27 November 2013

particles, more craze and formed and more energy can be absorbed. Furthermore, there were also more interact forces such as hydrogen bonding and Vander Waals interaction between the epoxy resin and nanoparticles of the epoxy coatings can be enhanced by nano modification.

4. Conclusions

The present study involves the development and characterisation of modified epoxy resin with a nano zinc oxide (ZnO) additive. The nano additive of different weight percentages was loaded with epoxy resin to formulate nano-hybrid coatings. The coated panels were evaluated for their corrosion resistance by means of electrochemical impedance studies, solvent rub test and salt spray test. The fouling resistance of these coatings was determined by antifouling studies subjecting the coated specimens in sea water for a period of 12 months at east coast of India, Tamilnadu, Chennai (Muttukadu boat house).

The nano-hybrid coating containing 2.5wt% of nZnO had shown excellent adhesion, impact resistance and flexibility which meet the requirements of a high performance coating. This is mainly attributed to the uniform distribution of nZnO (2.5wt %) within the epoxy matrix offering improved coating properties ideally suitable for corrosion and fouling prevention.

The data resulted from corrosion studies clearly indicate that the metal oxide like nZnO used in optimum wt% as antifoulant showed superior antifouling efficiency than the other coatings. It can be concluded that the nZnO of optimum wt% may be used as an effective antifouling biocide in coatings.

ISSN 1466-8858 Volume 16, Preprint 68 submitted 27 November 2013

Hence, we conclude that the barrier performance of epoxy coatings can be enhanced substantially by the incorporation of a second nano phase inorganic filler particles that should be dispersed uniformly within the epoxy resin to form an epoxy nanocomposite coating, by decreasing the porosity and restrain the diffusion path for deleterious species. The incorporation of nZnO particles into epoxy resins also offers environmentally benign solutions by enhancing the integrity and durability of epoxy coatings by filling cavities and cause crack bridging, crack deflection and crack bowing leading to better performance and longevity than the conventional epoxy coatings that are currently in use.

Acknowledgment

Instrumentation facility provided under FIST-DST and DRS-UGC to Department of Chemistry, Anna University, Chennai are gratefully acknowledged.

ISSN 1466-8858 Volume 16, Preprint 68 submitted 27 November 2013

References

[1] D.M. Yebra, S. Kiil, K. Dam-Johansen, Prog. Org. Coat. 50 (2004) 75–104.

[2] Ji.Wei-gang, Hu. Ji-Ming, Liu.Liang, Jian-Qing Zhang, Chu, Prog. Org. Coat. 57 (2006) 439-443.

[3] S. Bonati, F. Monteleone, Biocidal-Antifouling Agents with Low Eco toxicity Index. International Application Publication. Publication No. WO0128328, (2001)

[4] M.G.Hadfildk, V.J. Paul, Biofouling, 12 (2001) 9-29.

[5] D. Borisova, H. Mohwald, D.G. Shchukin, ACS Nano. 5 (2011) 1939-1946.

[6] C.C. Chang, T.Y. Oyang, F.H. Hwang, C.C. Chen, L.P. Cheng, J. Non-Cryst. Solids, 358 (2012)72–76.

[7] C.C. Chen, D.J. Lin, T.M, Don, F.H. Huang, L.P. Cheng, J. Non-Cryst. Solids. 354 (2008) 3828–3835.

[8] H. Miyagawa, M.J. Rich, L.T. Drzal, J. Polym. Sci. B. 42 (2004) 4384–4390.

[9] O. Becker, R. Varley, G. Simon, Polymer. 43(2002) 4365–4373.

[10] X. Shi, T.A. Nguyen, Z. Suo, Y. Liu, R. Avci, Surf. Coat. Technol. 204 (2009) 237– 245.

[11] M. Champ, The Science of the Total Environment. 258 (2000)21–71.

[12] S.I. Chang, K.A. Gray, Metal organic Interactions in Environmental Systems. 43(1) (2003) 529–30.

[13] J. Kim, I. Konstantinou, T. Albanis, Environment International. 30 (2004) 235–48.

[14] P. Miriam, B. Guillermo, G. Monica, A. Beatriz del, S. Mirta, Cupric tannate - A low copper content antifouling pigment. 44 (4) (2006) 311-315.

[15] L. Zhang, Y. Jiang, Y. Ding, M. Povey, D. York, J. Nanoparticle Res. 9 (3) (2010) 479- 489.

[16] S. Suwanboon, P. Amornpitoksuk, P. Bangrak, A. Sukolrat, J. Ceramic Processing Research. 11 (1) (2010) 547-551.

[17] N. Padmavathy, V. Rajagopalan, Sci. Technol. Adv. Mater. 9 (2008) 035004-11.

ISSN 1466-8858 Volume 16, Preprint 68 submitted 27 November 2013

[18] M. Auffan, J. Rose, J.Y. Bottero, G.V. Lowry, J.P. Jolivet, M.R. Wiesner, Nature Nanotechnol.4 (2009) 634-41.

[19] Y. Diego Meseguer, K. Soren, E. Claus, Weinell, J. Kim Dam, Prog. Org. Coat. 56 (2006) 327-337.

[20] R. Delio, R. Dordick, Biotechnology Progress.18 (2002) 551–5.

[21] M. Banoee, S. Seif, Z.E. Nazari, P. Jafari-Fesharaki, H.R. Shahverdi, A. Moballegh, K.M. Moghaddam, A.R. Shahverdi, E publication. 11 (3) (2010) 77-79.

[22] Shailesh K. Dhoke, A.S. Khanna, Prog. Org. Coat. 74 (2012) 92-99.

[23] Shailesh K. Dhoke, A.S. Khanna, Materials chemistry and physics. 117(2009) 550–556.

[24] J.M. Yang, H.T. Lin, W.C. Lai, J. Membr. Sci. 208 (2002) 105.

[25] C.Y. Bai, X.Y. Zhang, J.B. Dai, C.Y. Zhang, Prog. Org. Coat. 59 (2007) 331.

[26] S. Subramani, J.M. Lee, I.W. Cheong, J.H. Kim, J. Appl. Polym. Sci. 98 (2005) 620

[27] M. Ayman, F. Ahmed, E.I. Kafrawy, H. Morsy, A. Abdel-Azim, Prog. Org. Coat. 58 (2007)13–22.

[28] A. Sharif, F. Naqvi, S. Eram, L.V. Kanak, Prog. Org. Coat. 55 (2006) 268-275.

[29] S. Ananda Kumar, T. Balakrishnan, M. Alagar, Z. Denchev, Prog. Org. Coat. 55 (2006) 207–217.

[30] M. Berndt, C.C. Berndt, S.D. Cramer, B.S. Covino, Corrosion - Fundamentals, Testing and protection, ASM international, USA 13 (2003).

[31] M.R. Bagherzadeh, F. Mahdavi, Prog. Org. Coat. 60 (2007)117–120.

[32] C.F. Dong, H. Sheng, An, YH, Li, XG, K. Xiao, Y.F.Cheng, Prog. Org. Coat. 67 (2010) 269–273.

[33] S.L. Sinebryukhov, A.S. Gnedenkov, D.V. Mashtalyar, S.V. Gnedenkov, Surf. Coat. Technol. 205(2010) 1697–1701.

[34] N. Pebere, T. Picaud, M. Duprat, F. Dabosi, Corros. Sci. 29 (1989)1073–1086.

[35] F. Mansfeld, J. Appl. Electrochem. 25(1995) 187–202.

[36] S. Ananda Kumar, T.S.N. Sankara Narayanan, Prog. Org. Coat. 45(2002) 323–330.

ISSN 1466-8858 Volume 16, Preprint 68 submitted 27 November 2013

[37] T.S.N. Sankara Narayanan, M. Subbaiyan, Met. Finish. 92 (9) (1994)33–36.

[38] Y. Okazaki, Biomaterials, 23 (2002) 2071–2077.

[39] F. Louis Floyd, S. Avudiappan, J. Gibson, B. Mehta, P. Smith, T. Provder, J. Escarsega, Prog. Org. Coat. 66 (1) (2009)8–34.

[40] K. Hladky, L.M. Callow, J.L. Dawson, Brit. Corros.15 (1980) 20–25.

[41] S. Ananda Kumar, A. Sasi Kumar, Prog. Org. Coat. 68 (3) (2010) 189–200.

[42] ASTM D3623, Standard Test Method for Testing Antifouling Panels in Shallow Submergence, (2004).

[43] F. Fabienne, L.Isabelle, L. Valerie, H. Dominique, V.R. Karine, Prog. Org. Coat. 54 (2005) 216–223.

[44] S.K. Dhoke, A.S. Khanna, T.J. Mangal Sinha, Prog. Org. Coat. 64 (2009) 371–82.

[45] K.M. Aswini, M. Rama Shanker, N. Ramanuj, K.V.S.N. Raju, Prog. Org. Coat.67 (2010) 405–413.

[46] C. Marieta, G. Remiro, G. Garmendia, I. Harismendy, I. Mondragón, rphologies in toughened thermosetting matrices. European Polymer Journal. ISSN 0014-3057 39 (10) (2003)1965-1973.

[47] G. Nikolic, S. Zlatkovic, M. Cakic, S. Cakic, C. Lacnjevac, Z. Rajic, Sensors, ISSN 1424-8220. 10 (1) (2010) 684-696.

[48] B. Ramezanzadeh, M.M. Attar, M. Farzam, J. Therm. Anal. Calorim. 103(2011) 731–739.

[49] A. Rigail-Ceden, C.S.P. Sung, Polymer. 46 (2005)9378-9384.

[50] J.M. Chalmers, N.J. Everall, M.D. Schaeberle, I.W. Levin, E.N. Lewis, L.H. Kidder, J. Wilson, R. Crocombe, Vib. Spectrosc. 30 (2002) 43-49.

[51] N. Poisson, G. Lachenal, H. Sautereau, Vib. Spectrosc.12 (1996)237-247.

[52] J. Mijovic, S. Andjelic, Polymer, 37 (1996) 1295-1303.

[53] C. Billaud, M. Vandeuren, R. Legras, v. Carlier, J. Appl. Spectrosc. 56 (2002) 1413-1421.

ISSN 1466-8858 Volume 16, Preprint 68 submitted 27 November 2013

[54] S. Zlatkovic, G.S. Nikolic, J. Stamenkovic, Chem. Ind. (Serb.) 57 (2003) 563-567.

[55] K. Krzysztof, S. Tadeusz, Prog. Org. Coat. 62 (2008) 425-429.

[56] R. Selvaraj, M. Selvaraj, S.V. Iyer, Prog. Org. Coat. 42(2009) 454-459.

[57] M.A. Ayman, M.I. Abdou, A. Abdel, A. Elsayed, E. Mohamed, Prog. Org. Coat. 63 (2008) 372-376.

[58] S.M. Krishnan, Prog. Org. Coat. 57 (2006) 383-391.

[59] K. Lam, K.T. Lau, Compo. Struc. 75 (2006) 553-558.

[60] A. Hartwig, M. Sebald, D. Putz, L. Aberle, Macromol. Symp. 221(2005) 127-136.

[61] F. Dietsche, Y. Thomann, R. Thomann, R.Mulhaupt, J. Appl. Polym. Sci. 75 (2000) 396- 405.

[62] M.A. Ayman, N.O. Shanker, M.I. Abdou, M. Abdelfatah, Prog. Org. Coat. 56 (2006) 91-99.

[63] M. Arthananareeswari, T.S.N. Sankara Narayanan, P. Kamaraj, M. Tamilselvi, J. Coat. Technol. Res, 9(1) (2012) 39-46.

[64] S. Ananda Kumar, M. Alagar, V. Mohan, JMEPEG. 11(2002) 123-129.

[65] S. Ananda Kumar, M. Alagar, V. Mohan, Surface Coatings International Part B: Coatings Transactions, 84(2001) 43-48.

[66] L.N. Pedro de, P.A. Alexsander, S.A. Walney, N.C. Adriana, Prog. Org. Coat. 62 (2008) 344-350.

[67] S. Anandakumar, A novel epoxy coatings for corrosion and fouling resistance, in - Proceedings of Coatings Science International Conference, COSi, (2009).

[68] M. Chen, Y. Qu, L. Yang, H. Gao, Structures and antifouling properties of low surface energy non-toxic antifouling coatings modified by nano-SiO_2 powder, Science in China Series B—Chemistry 51 (2008) 848.

JCSE The Journal of Corrosion Science and Engineering
ISSN 1466-8858 Volume 16, Preprint 68 submitted 27 November 2013

Figure Captions

Fig.1. The Preparation Process of Nano hybrid Coating

Fig.2. (a) EIS test apparatus (b) Equivalent circuit models for paint coated mild steel

Fig.3. FTIR of (a) Coating '1', (b) Coating '2', (c) Coating '3', (d) Coating '4', (e) Coating '5' and (f) Nano ZnO

Fig.4. Polarization response of different coating systems for 0 Days of immersion in 3.5% NaCl solution. (a) Uncoated (b) Coating '1' (c) Coating '2' (d) Coating '3' (e) Coating '4' (f) Coating '5'

Fig.5. Bode plot of different coating systems for 0 days of Immersion in 3.5% NaCl solution. (a) Uncoated (b) Coating '1' (c) Coating '2' (d) Coating '3' (e) Coating '4' (f) Coating '5'

Fig.6. Salt-spray test result of coating systems after 1200 h exposure of 3.5% NaCl: (a) Photograph of coating panels before salt-spray test (b) Photograph of coating panels after 1200 h in 3.5% NaCl Solution

Fig.7. Photos taken after the panels were immersed in seawater: (a) Photograph of coating panels after 6^{th} month's immersion in seawater (b) Photograph of coating panels after 12^{th} month's immersion in seawater.

Fig.8. SEM image taken before and after the panels were immersed in seawater: (a) SEM images of coating panels 0 days immersion in seawater (b) SEM images of coating panels after 12^{th} month's immersion in seawater.

Fig.9. Forming process of the coating films

JCSE The Journal of Corrosion Science and Engineering
ISSN 1466-8858 Volume 16, Preprint 68 submitted 27 November 2013

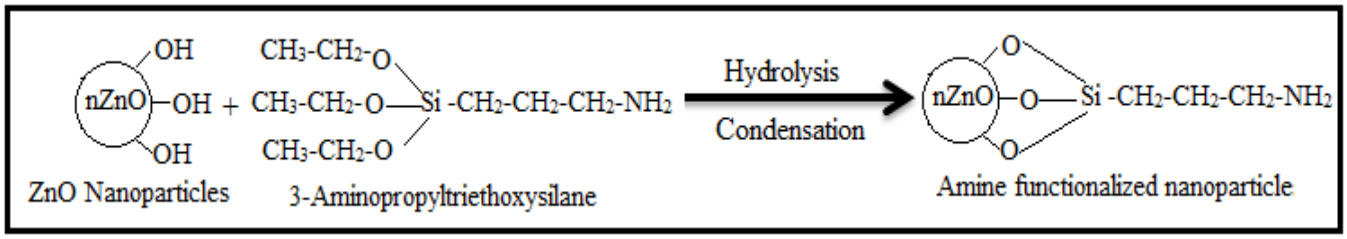

Scheme: 1 Surface modification of nonmaterial

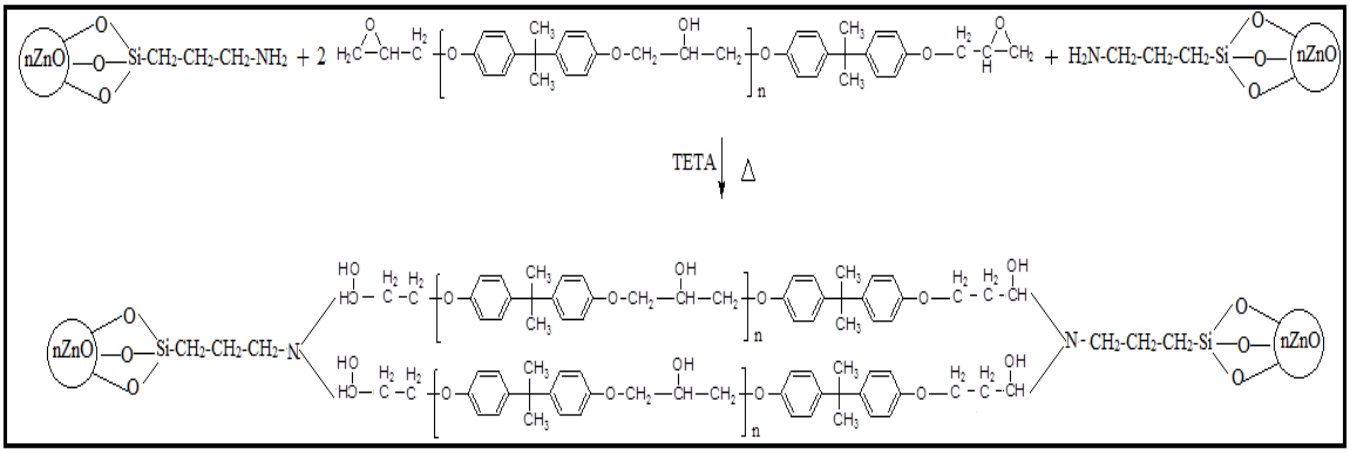

Scheme 2: The Schematic formula for the reaction between epoxy resin and surface modified ZnO nanoparticle.

JCSE The Journal of Corrosion Science and Engineering
ISSN 1466-8858 Volume 16, Preprint 68 submitted 27 November 2013

Figure 1

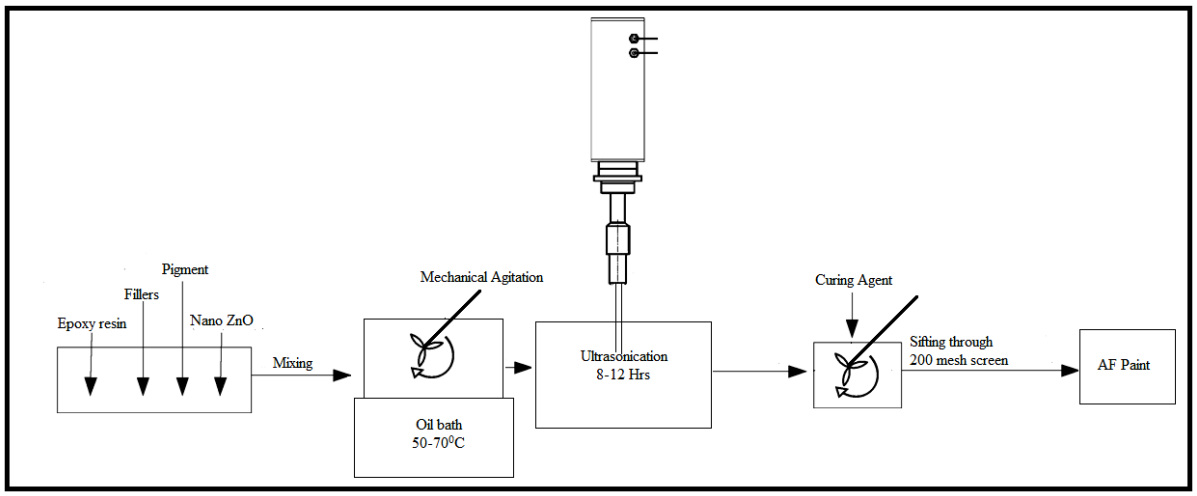

JCSE The Journal of Corrosion Science and Engineering
ISSN 1466-8858 Volume 16, Preprint 68 submitted 27 November 2013

Figure 2a

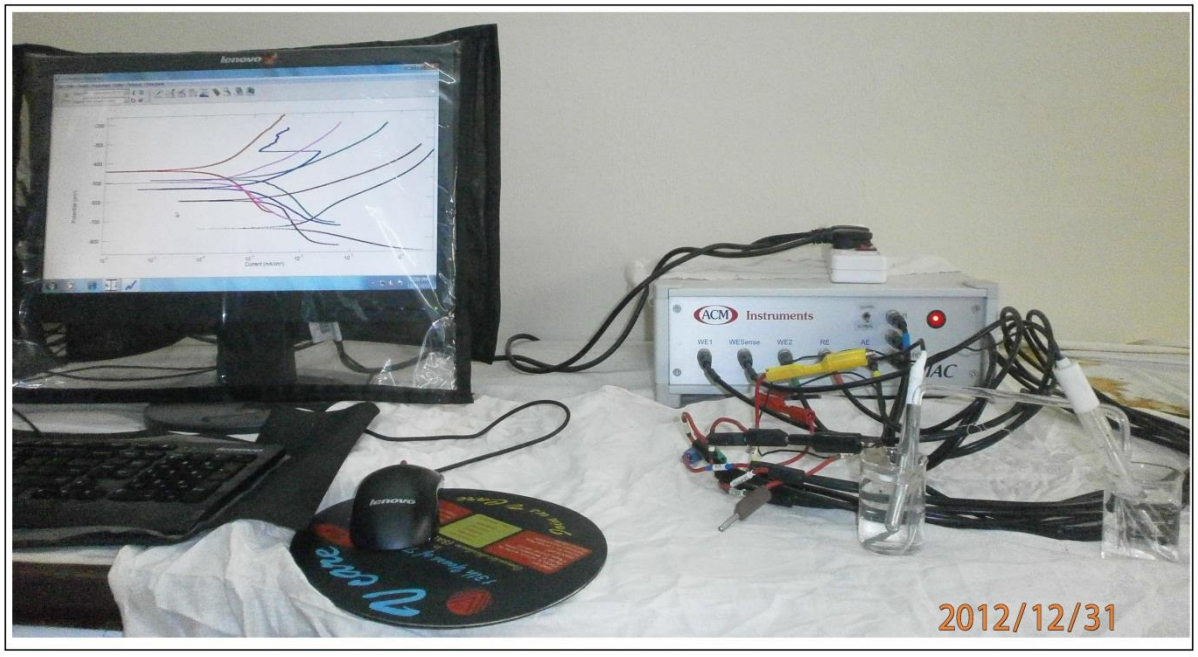

JCSE The Journal of Corrosion Science and Engineering
ISSN 1466-8858 Volume 16, Preprint 68 submitted 27 November 2013

Figure 2b

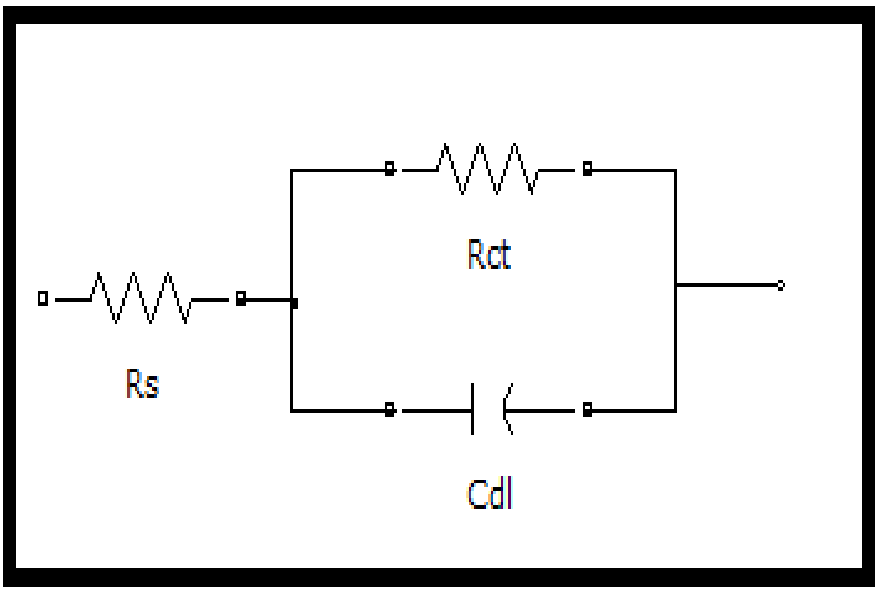

JCSE The Journal of Corrosion Science and Engineering
ISSN 1466-8858 Volume 16, Preprint 68 submitted 27 November 2013

Figure 3

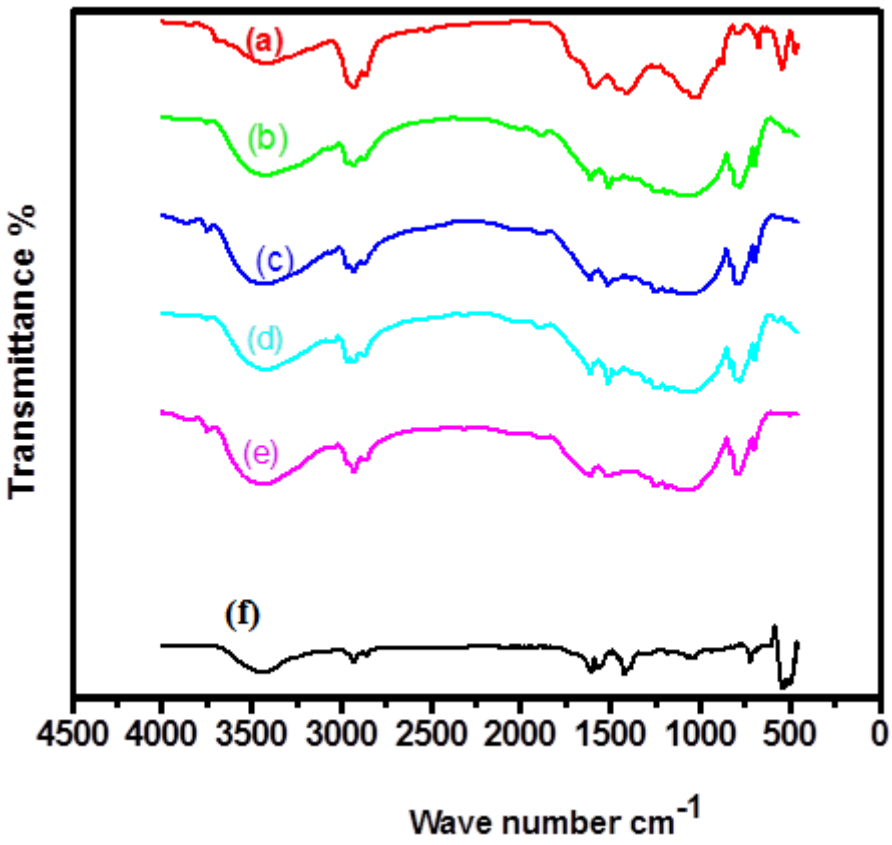

JCSE The Journal of Corrosion Science and Engineering
ISSN 1466-8858 Volume 16, Preprint 68 submitted 27 November 2013

Figure 4

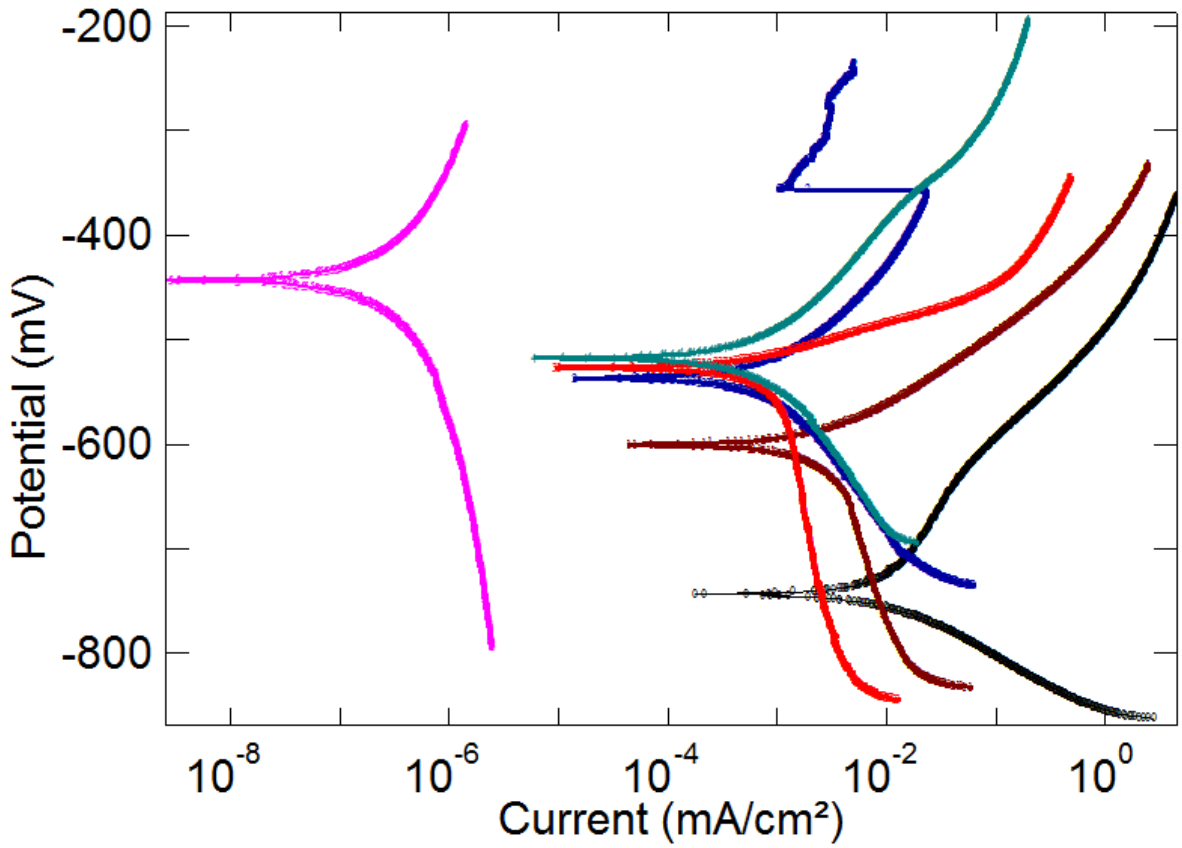

JCSE The Journal of Corrosion Science and Engineering
ISSN 1466-8858 Volume 16, Preprint 68 submitted 27 November 2013

Figure 5

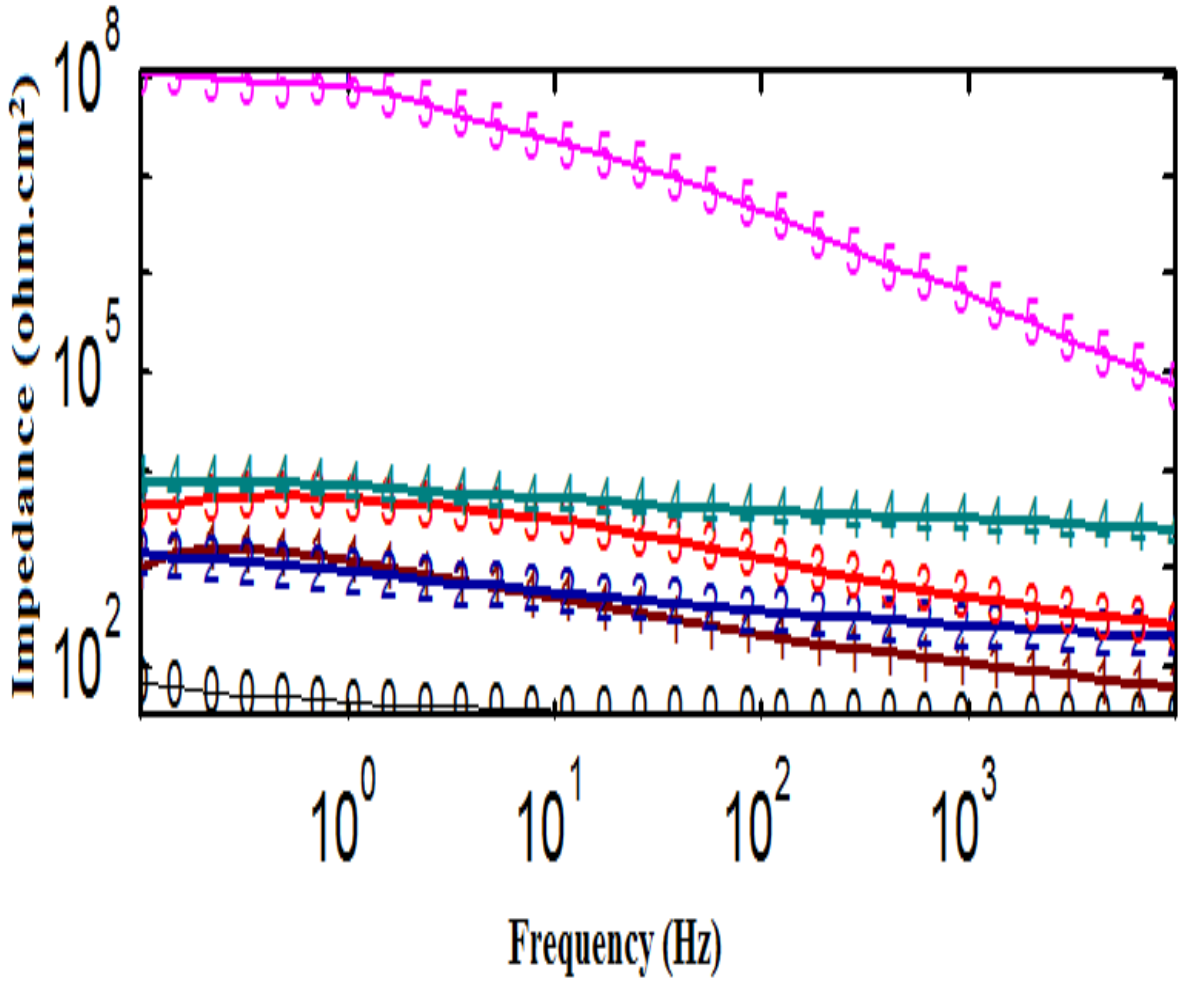

JCSE The Journal of Corrosion Science and Engineering
ISSN 1466-8858 Volume 16, Preprint 68 submitted 27 November 2013

Figure 6

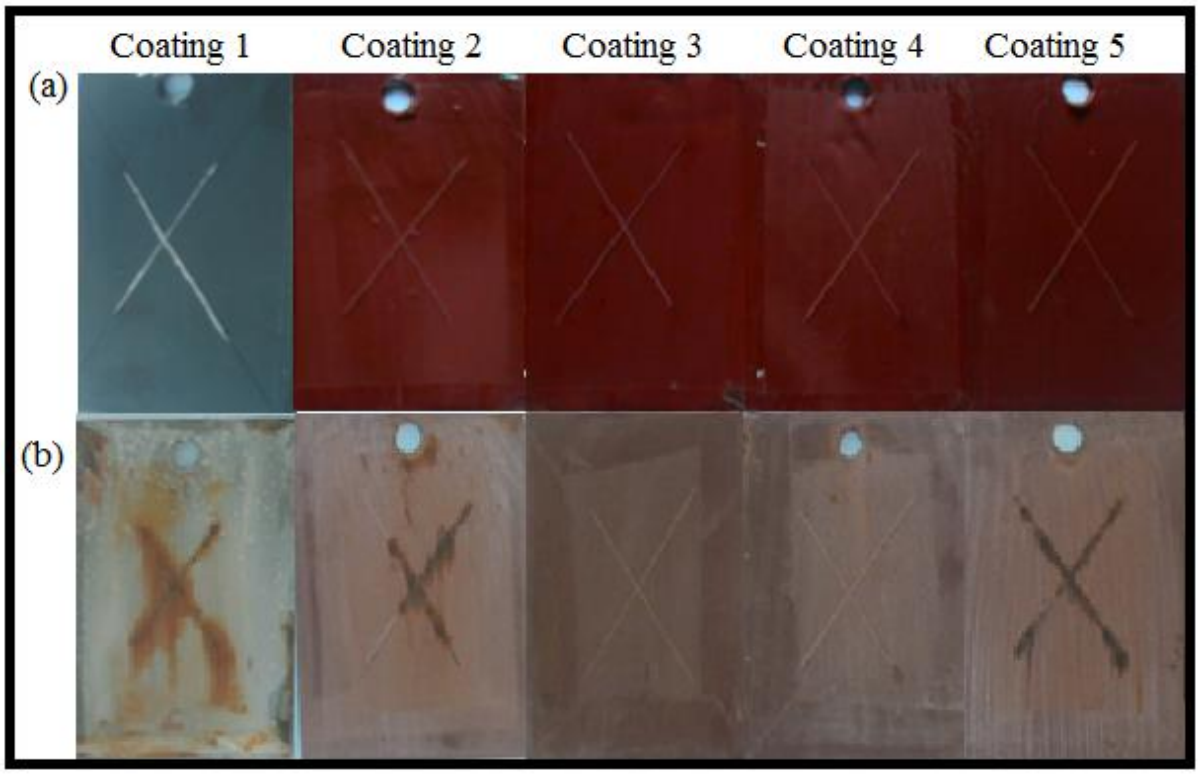

JCSE The Journal of Corrosion Science and Engineering
ISSN 1466-8858 Volume 16, Preprint 68 submitted 27 November 2013

Figure 7

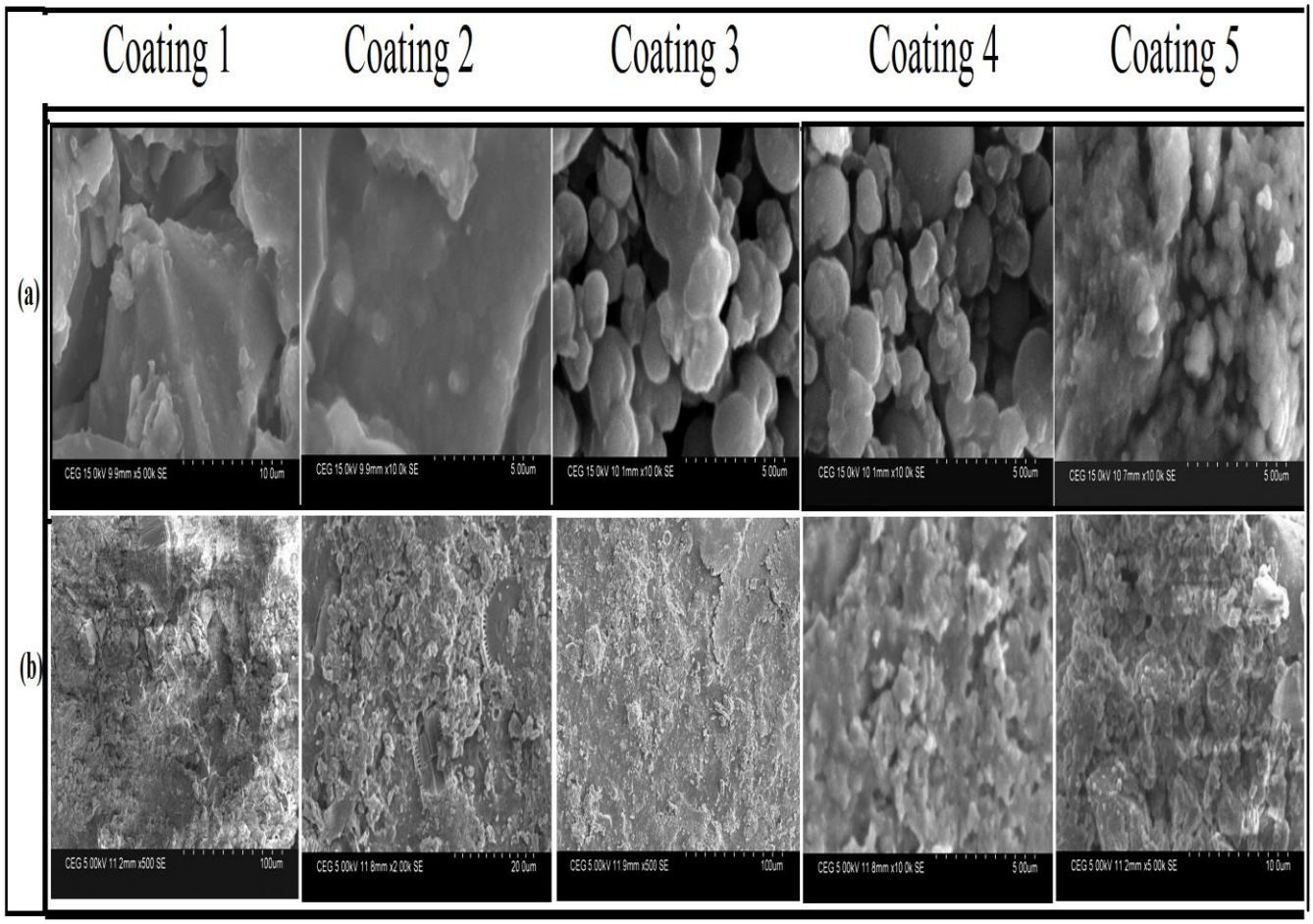

JCSE The Journal of Corrosion Science and Engineering
ISSN 1466-8858 Volume 16, Preprint 68 submitted 27 November 2013

Figure 8

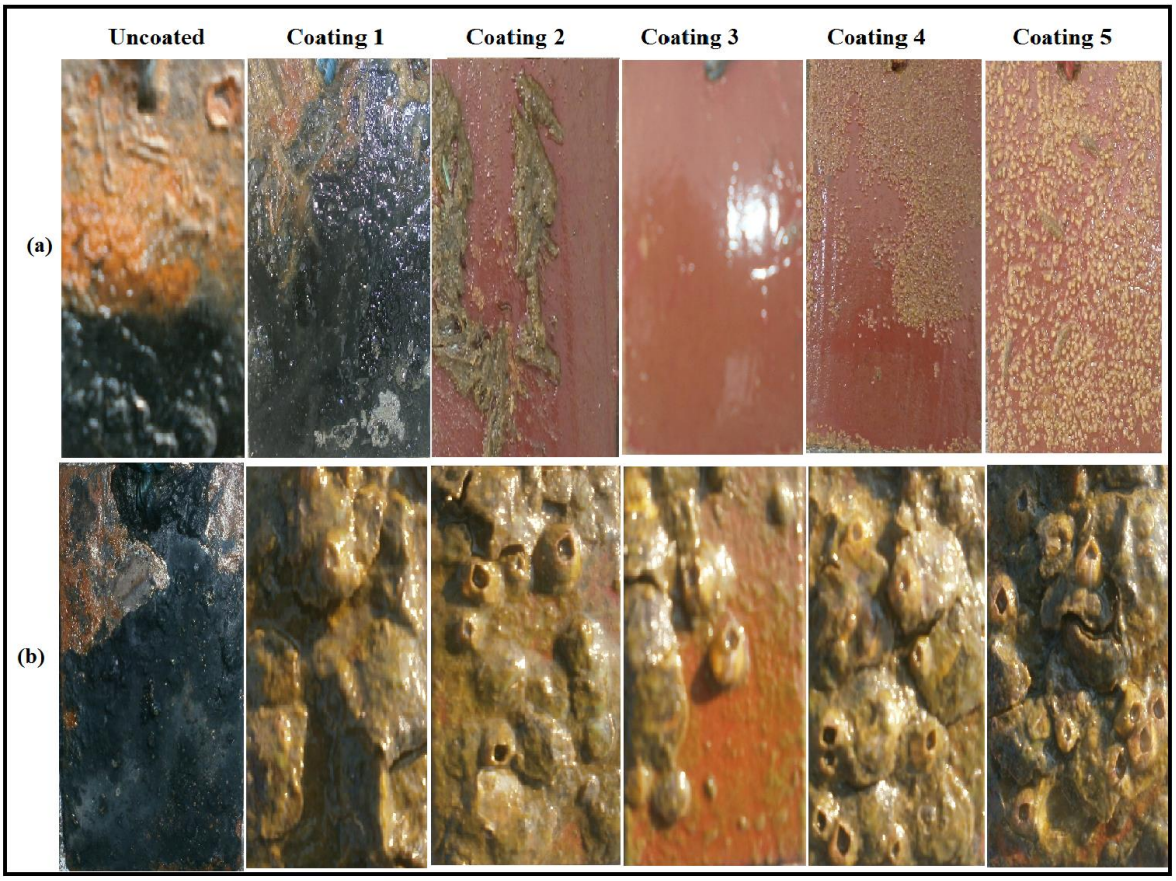

JCSE The Journal of Corrosion Science and Engineering
ISSN 1466-8858 Volume 16, Preprint 68 submitted 27 November 2013

Figure 9

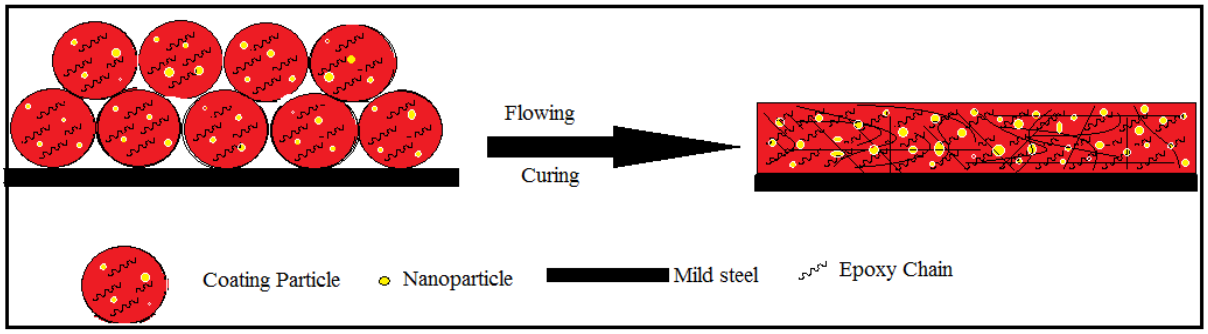

JCSE The Journal of Corrosion Science and Engineering
ISSN 1466-8858 Volume 16, Preprint 68 submitted 27 November 2013

Table 1.

Nomenclature of coating system on mild steel

Coating System	Epoxy Resin	Additives					
		Pigment	Extender	Surface modified nZnO			curing agent
				2.5%	5.0%	7.5%	
Uncoated	×	×	×	×	×	×	×
Coating 1	DGEBA	×	×	×	×	×	TETA
Coating 2	DGEBA	✓	✓	×	×	×	TETA
Coating 3	DGEBA	✓	✓	✓	×	×	TETA
Coating 4	DGEBA	✓	✓	×	✓	×	TETA
Coating 5	DGEBA	✓	✓	×	×	✓	TETA

JCSE The Journal of Corrosion Science and Engineering
ISSN 1466-8858 Volume 16, Preprint 68 submitted 27 November 2013

Table 2.

Mechanical characterization of Nano-hybrid coating systems on mild steel

Coating Systems	Average dry film thickness (µm)	Impact resistance (Weight 1.8kg and height of fall 1.2m)	Flexibility	Cross-Cut adhesion test	Water Absorption (%)	Gel Content (%)
Coating 1	±100	No damage	Passed (6mm)	5B	12.5	47.5
Coating 2	±100	No damage	Passed (3mm)	5B	11.4	50.2
Coating 3	±100	No damage	Passed (3mm)	5B	9.4	63.3
Coating 4	±100	No damage	Passed (3mm)	5B	7.3	77.4
Coating 5	±100	No damage	Passed (3mm)	5B	5.2	92.5

JCSE The Journal of Corrosion Science and Engineering
ISSN 1466-8858 Volume 16, Preprint 68 submitted 27 November 2013

Table 3.

Solvent and chemical resistance tests of Nano hybrid coating systems on mild steel

Coating System	Distilled Water (WL[b], mg) 96h	5% H_2SO_4 (WL[b], mg) 96h	5% NaOH (WL[b], mg) 96h	Aceton[a] (DRs)
Uncoated	0.0193	0.3988	0.4005	-
Coating 1	A	C	C	>25
Coating 2	A	B	B	>27
Coating 3	A	B	B	>27
Coating 4	A	B	B	>27
Coating 5	A	B	B	>27

Film appearance: A-no effect; B-Slight loss of gloss, film intact; C- Loss of gloss, film intact; D-blistering
[a]DRs: Film appearance affected after specified double rubs.
[b]WL: weight loss.

JCSE The Journal of Corrosion Science and Engineering
ISSN 1466-8858 Volume 16, Preprint 68 submitted 27 November 2013

Table 4

Data resulted from Tafel study after 60 days of immersion in 3.5% NaCl

Coating System	Ecorr mv	LPR Ohm.cm^2	βa mv	βc mv	Icorr mA/cm^2	CR mm/y
Uncoated	-741.8	123.5	137	56	8.8857×10^{-3}	1.0298×10^{-1}
Coating 1	-600	268	53	113	1.7910×10^{-3}	2.0767×10^{-2}
Coating 2	-536	9938	91	123	8.087×10^{-4}	9.3727×10^{-3}
Coating 3	-442	1.325×10^{3}	100	92	1.291×10^{-7}	1.4960×10^{-6}
Coating 4	-517	2488	60	64	3.288×10^{-4}	3.8113×10^{-3}
Coating 5	-534	3666	76	126	2.221×10^{-3}	2.5744×10^{-3}

JCSE The Journal of Corrosion Science and Engineering
ISSN 1466-8858 Volume 16, Preprint 68 submitted 27 November 2013

Table 5

Data resulted from impedance study after 60 days of immersion in 3.5% NaCl

Coating System	I_{Corr} mA/cm^2	C_R mm/y	Rs Ohm.cm^2	R_{ct} Ohm.cm^2	C_{dl} F/cm^2
Uncoated	5.428×10^{-1}	6.291×10^{-1}	3.221×10^{3}	4.806×10^{1}	2.282×10^{-2}
Coating 1	2.187×10^{-2}	2.534×10^{-1}	6.337×10^{1}	1.193×10^{3}	5.903×10^{-5}
Coating 2	2.019×10^{-2}	2.340×10^{-1}	2.264×10^{2}	1.292×10^{3}	3.822×10^{-4}
Coating 3	2.436×10^{-7}	2.823×10^{-6}	1.324×10^{4}	1.071×10^{8}	2.576×10^{-9}
Coating 4	4.612×10^{-3}	5.346×10^{-2}	2.469×10^{3}	5.656×10^{3}	1.955×10^{-5}
Coating 5	1.772×10^{-3}	2.054×10^{-2}	1.439×10^{3}	1.472×10^{4}	4.276×10^{-5}

JCSE The Journal of Corrosion Science and Engineering
ISSN 1466-8858 Volume 16, Preprint 68 submitted 27 November 2013

Table 6.

Results of salt spray (fog) test

Coating System	Observation after 600h	Observation after 1200h
Coating 1	pale yellow rust along the scribes, no blistering, no chalking	light brown rust along the scribes, rust creep 2mm along scribes
Coating 2	no pale yellow rust along the scribes, no blistering, no chalking	light brown rust along the scribes, rust creep 1mm along scribes
Coating 3	no pale yellow rust along the scribes, no blistering, no chalking	no light brown rust along the scribes, no rust creep
Coating 4	no pale yellow rust along the scribes, no blistering, no chalking	no light brown rust along the scribes, no rust creep
Coating 5	no pale yellow rust along the scribes, no blistering, no chalking	light brown rust along the scribes, rust creep 2mm along scribes